Level Set Segmentation of Cellular Images Based on Topological Dependence

Weimiao Yu[1], Hwee Kuan Lee[1], Srivats Hariharan[2], Wenyu Bu[2], and Sohail Ahmed[2]

[1] Bioinformatics Institute, #07-01, Matrix, 30 Biopolis Street, Singapore 138671
[2] Institute of Medical Biology, #06-06, Immunos, 8A Biomedical Grove, Singapore 138648

Abstract. Segmentation of cellular images presents a challenging task for computer vision, especially when the cells of irregular shapes clump together. Level set methods can segment cells with irregular shapes when signal-to-noise ratio is low, however they could not effectively segment cells that are clumping together. We perform topological analysis on the zero level sets to enable effective segmentation of clumped cells. Geometrical shapes and intensities are important information for segmentation of cells. We assimilated them in our approach and hence we are able to gain from the advantages of level sets while circumventing its shortcoming. Validation on a data set of 4916 neural cells shows that our method is $93.3 \pm 0.6\%$ accurate.

1 Introduction and Background

Biological science is in the midst of remarkable growth. Accompanying this growth is the transformation of biology from qualitative observations into a quantitative science. This transformation is driving the development of bio-imaging informatics. Computer vision techniques in bio-imaging informatics have already made significant impacts in many studies [1,2]. Cellular microscopy is an important aspect of bio-imaging informatics. It have its unique traits and bring new challenges to the field of computer vision. Advances in digital microscopy and robotic techniques in cell cultures have enabled thousands of cellular images to be captured through High Throughput Screening and High Content Screening. Manual measurement and analysis of those images are subjective, labor intensive and inaccurate. In this paper, we developed an efficient algorithm for the segmentation of cells in highly cluttered environment, which is a ubiquitous problem in the analysis of cellular images.

Accurate segmentation of the cellular images is vital to obtain qualitative information on a cell-by-cell basis. Cellular images are usually captured by multichannel fluorescent microscopes, in which one channel detects the nuclei. Since nuclei contain important information, they generally serve as references for cellular image segmentation. During the past 15 years, many efforts have been made on automatic segmentation of nuclei from fluorescent cellular images, such as

G. Bebis et al. (Eds.): ISVC 2008, Part I, LNCS 5358, pp. 540–551, 2008.

simple thresholding [3], watershed algorithm [4]∼[5], boundary based segmentation [6], flexible contour model for the segmentation of the overlapping and closely packed nucleus [7]. Other related works on the automatic analysis of cellular images can be found in [8,9].

Deformable models, also known as active contour, are popular and powerful tools for cell segmentation tasks. Among all the active contour models, level set formalism has its superior properties, such as ease of implementation, region-based, robust to noise and no self-intersection, *etc.* Two concepts of level set approach were discussed in O. Stanley's original paper [10]. First, a level set function in a higher dimensional space is defined to represent the regions, which provided us with a non-parameterized model for segmentation. Second, the curves are evolved according to their mean curvature. Thereafter, D. Mumford and J. Shah proposed their functional variation formulation to optimize the segmentation of piecewise smooth images in [12]. Then Chan-Vese enhanced the level set approach for region based image segmentation [13]. A comprehensive review of level set approach for image processing are available in [14] and [15].

One long-claimed merit of level set methods is its ability to automatically handle topological changes. However, this merit becomes a liability in many cellular image segmentations, because non-dividing cells can only contain one nucleus. In a highly clustered image, as shown in Fig. 1, level set segmentation of the cells (green channel) will results in many segments with multiple nuclei. The contours of the snake model and geodesic active contours model can in principle generate one cell segment per nucleus, but they need to be parameterized and the node points may not be uniformly distributed along the length of the contours. Thus they cannot capture the subtle details of irregular cell outlines. In this work, we prefer the level set formulation since it is non-parameterized. We develop a method to enforce the condition that one cell segment contains only one nucleus.

Watershed approach was first proposed in [16] and widely applied for cell segmentation. Watershed approach was combined with the level set formulation to segment cellular images and preserve the known topology based on sought seeds in [17]. Similar seeds-based segmentation approach in [18] uses one level set function for each individual corresponding cell to prevent the merging of different cells. Simple point concept is applied to prevent the merging of the cell segments during the evolution of level set function in [19]. However, a well-known problem of watershed approach is over-segmentation. Other methods have been proposed to overcome this problem, such as rule-based merging [21] and marker-controlled watershed correction based on Voronoi diagrams [20].

Generally, the cellular images are acquired by multi-channel fluorescent microscopes and nuclei are captured by one of the channels. Fig. 1 shows a few examples of the cellular images captured by two channel fluorescent microscopy. As shown in Fig. 1, each cell consists of one nucleus and cells of irregular shapes are crowded and touch each other. In this work, we first segment the nuclei, since they are inside of the cell membrane and generally well separated. The found nuclei serve as *seeds* for cell segmentation. We present a novel cell segmentation approach based on the concept of topological dependence, which will

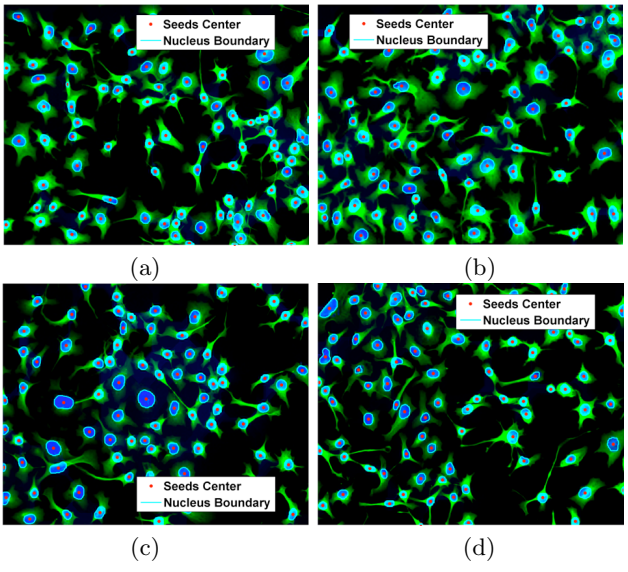

Fig. 1. Captured cellular images with detected nuclei. Detected seeds are outlined in blue and the geometric centers are marked by red dots.

be introduced shortly. In our approach, the level set curves propagate faster in the regions of brighter image intensities. Hence the dynamics of the level set curves incorporate essential information for cell segmentation. The utilization of such dynamics in our approach is presented for the first time in literature. The watershed lines are evolved dynamically based on the topological dependence at each time step to segment the crowded cells with irregular morphology.

The remainder of the paper is structured as follows. Section 2 will provide the definition of topological dependence. The level set formulation for two phase segmentation will be presented in the length of Section 3. The dynamic watershed transformation and the topological dependence preservation will be discussed in Section 4. In Section 5, we will present our experimental results. The conclusion in Section 6 will finalize this paper.

2 Topological Dependence

In this paper, we use the images of two channels to illustrate our approach. Generalization of our approach to the images of more than two channels is trivial as long as we use one channel as reference. The nucleus is stained in blue and cell cytoplasm is stained in green. We define the images on a finite subset in the two dimensional Euclidean space $\mathbf{\Omega} \subset \mathbb{R}^2$. $f^n(x,y) : \mathbf{\Omega} \to \mathbb{R}$ and $f^c(x,y) : \mathbf{\Omega} \to \mathbb{R}$ represent the intensities of nucleus and cytoplasm at (x,y) respectively. We call $f^n(x,y)$ and $f^c(x,y)$ *Nucleus Image* and *Cell Image*. The superscripts *'n'* and *'c'* represent 'nucleus' and 'cell'. Both of the functions are normalized to $[0,1]$.

The segments of nucleus and cell images form connected regions in $\mathbf{\Omega}$. Due to the limitation of space, we give a brief statement to define the connected region:

> **Connected region:** *A set of points $\pi \subseteq \mathbf{\Omega}$ form a connected region if for any two different points $(x_1, y_1) \in \pi$ and $(x_2, y_2) \in \pi$, there exists a path Γ connecting (x_1, y_1) and (x_2, y_2) such that $\Gamma \subseteq \pi$.*

The segmentation of nucleus is relatively easy, since they are better separated. After the segmentation of nuclei, we obtain a set of connected regions, *e.g.* segments of nuclei, denoted by ω_i^n,where $i = 1, 2, ...L$. The topology of the nuclei is then determined. Each cell segment should contain exactly one nucleus segment. In order to describe this constraint in a rigorous mathematical framework, we introduce the concept of topological dependence:

> **Topological dependence:** *a set of connected regions π_i, $i = 1, 2, ...L$ is said to be topologically dependent with another set of connected regions θ_i, $i = 1, 2, ...L$ if:*

$$\theta_i \subseteq \pi_i \qquad i = 1, 2, ...L \tag{1}$$

Note that our definition of topological dependence is different from homeomorphism[11]. Topological dependence is more relaxed. Due to the limitation of space, we will not discuss in details here.

3 Level Set Segmentation

Mumford-Shah model of level set formalism is applied to obtain the segmentation of nucleus images and the cell images, which is given by [12]:

$$\begin{aligned} E(\phi, c_1, c_2) =& \mu \cdot length\{\phi = 0\} + \nu \cdot area\{\phi \geq 0\} \\ &+ \lambda_1 \int_{\phi \geq 0} |u(x, y) - c_1(\phi)|^2 dxdy \\ &+ \lambda_2 \int_{\phi < 0} |u(x, y) - c_2(\phi)|^2 dxdy \end{aligned} \tag{2}$$

where $u(x, y)$ is the image intensity. μ, ν, λ_1 and λ_2 are parameters to regularize the contour length, area, foreground and background respectively. c_1 and c_2 are constants to be determined through the optimization. They are determined by $c_1 = \frac{\int_{\phi \geq 0} u(x,y) dxdy}{\int_{\phi \geq 0} dxdy}$ and $c_2 = \frac{\int_{\phi < 0} u(x,y) dxdy}{\int_{\phi < 0} dxdy}$. In our work, the length and area parameters μ and ν are set to zero in order to allow irregular contours and varying sizes of nuclei and cells. In general, we may set the parameters accordingly when *a priori* knowledge on the length and area are available.

The optimal solution of Mumford-Shah model is given by the Euler-Lagrange equation, which is an iterative procedure:

$$\phi^{t+\Delta t} = \phi^t + \Delta t \cdot \delta_\varepsilon [-\lambda_1 (u(x, y) - c_1(\phi^t))^2 + \lambda_2 (u(x, y) - c_2(\phi^t))^2] \tag{3}$$

t is the artificial time used for the evolution of the level set function and Δt is the time step. δ_ϵ is a regularized delta function defined in [13]. The selection of the parameters is important to achieve a good segmentation. We will discuss the parameter selection on λ_1, λ_2 and Δt in more details in Section 5.

In order to segment the nuclei, we initialize the level set function for nucleus image as:

$$\phi^{n,t=0}(x,y) = f^n(x,y) - \frac{\int_{\mathbf{\Omega}} f^n(x,y)dxdy}{\int_{\mathbf{\Omega}} dxdy} \tag{4}$$

Substitute $u(x,y)$ by *Nucleus Image* $f^n(x,y)$ and then evolve the level set function $\phi^{n,t}$ using Eq.(3). After the iterations converged, the set of points $\{(x,y) \in \mathbf{\Omega} | \phi^{n,t}(x,y) \geq 0\}$ form L connected regions that define the nucleus segments ω_i^n, where $i = 1, 2, \cdots L$. L is the number of detected nuclei. The pixels belonging to ω_i^n are labeled by the integer i. All remaining pixels are labeled by 0 to represent the background. The detected nuclei will serve as *seeds* for the cell segmentation.

After the nuclei are segmented, we need to include the information of the nuclei into the cell segmentation. The level set function for the cell image segmentation is defined based on ω_i^n:

$$\phi^{c,t=0} = \hat{f}^c(x,y) - 1 \tag{5}$$

where,

$$\hat{f}^c(x,y) = \begin{cases} 1 & \text{if } (x,y) \in \bigcup_i^L \omega_i^n \\ f^c(x,y) & \text{otherwise} \end{cases} \tag{6}$$

Since $f^c \in [0,1]$, $\hat{f}^c(x,y) \in [0,1]$. Substitute $u(x,y)$ by $\hat{f}^c(x,y)$, then the level set function for the cell segmentation $\phi^{c,t}$ is evolved according to Eq.(3). Unlike the works in [18] where each individual cell has one corresponding level set function, we use only one level set function to segment all cells in order to achieve better computational efficiency.

In order to utilize the image intensity variation for cell segmentation, we initialize the level set function for cell segmentation according to Eq. (5) instead of traditional distance function. In addition, such initialization also ensures that the zero level sets start from the nuclei and evolve outwards with a speed related with the image intensity, *e.g.* brighter regions will be segmented as foreground earlier.

4 Preservation of Topological Dependence

The evolution of the level set function alone cannot ensure topological dependence between the cell segments and the nucleus segments. Dynamic watershed lines is applied to preserve such topological dependence. Let's define the segments of cells at time t as $\omega_i^{c,t}$. At $t = 0$, $\omega_i^{c,t=0}$ forms L connected regions. According to the definition of $\phi^{c,t=0}$, we know that $\omega_i^{c,t=0} = \omega_i^n$, $i = 1, 2, \cdots L$.

This indicates $\omega_i^{c,t=0}$ is topologically dependent with ω_i^n. Under the condition that $\omega_i^{c,t}$ is topologically dependent with ω_i^n at some time t, we may calculate the watershed lines W^t by:

$$W^t = \{(x,y) \in \mathbf{\Omega} : d_{\min}[(x,y)|\omega_i^{c,t}] = d_{\min}[(x,y)|\omega_j^{c,t}], \\ \text{for some } i \neq j, \text{where } i,j = 1,2,...L,\} \tag{7}$$

where:

$$d_{\min}[(x,y)|\omega^{c,t_i}] = \min_{(x',y') \in \omega_i^{c,t}} \sqrt{(x-x')^2 + (y-y')^2} \tag{8}$$

The obtained watershed line at time t will be used to preserve the topological dependence between $\omega_i^{c,t}$ and ω_i^n at time $t + \Delta t$.

Preserving topological dependence and recovering the correct segmentation consist of a series of re-labeling steps. Firstly, the connected regions that do not contain any nucleus segment are removed at each iteration, as shown by the gray region in Fig. 2(b). If the remaining connected regions is topologically dependent with ω_i^n, then these regions will take the labels of ω_i^n and we denoted them as the cell segments $\omega_i^{c,t+\Delta t}$.

If the topological dependence is violated, relabel the connected regions as "unknown" and the background as "0". Then, obtain the intersection of the

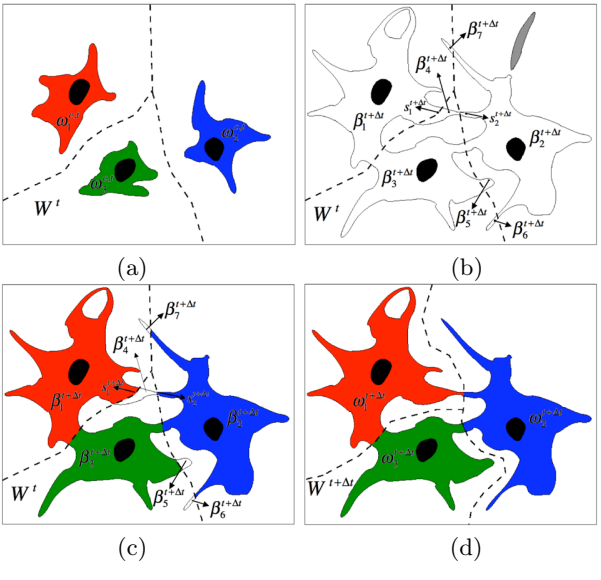

Fig. 2. Illustration of dynamic watershed lines and preservation of the topological dependence. Nucleus segments are black. Labels of different regions at different time are indicated by random colors. The dotted line represents the watershed line W^t. The level set function evolves from t in (a) to $t + \Delta t$ in (b). Thereafter re-labeling are carried out in (c) and (d) to eliminate the residual regions and preserve the topological dependence.

connected regions and W^t, which forms a set of common boundaries $\{s_1^{t+\Delta t}, s_2^{t+\Delta t}, \cdots\}$. Two of such common boundaries are illustrated by $s_1^{t+\Delta t}$ and $s_2^{t+\Delta t}$ in Fig. 2(b). Consider regions separated by the common boundaries as different connected regions, then we obtain a new set of connected regions $\beta_k^{t+\Delta t}$, $k = 1, 2, ...K$. (Note that $K \geq L$). If $\omega_p^n \subseteq \beta_q^{t+\Delta t}$, for some p and q, we label $\beta_q^{t+\Delta t}$ with the labels of ω_p^n. Not all $\beta_k^{t+\Delta t}$ can be re-labeled according to the above condition. Unlabeled regions are known as *residual regions*. An iterative procedure is given to find the correct labels of residual regions:

> **Re-labeling of the residual regions:** *Any residual region must be created by some common boundaries. One side of those common boundaries must be adjacent to this given residual region and the other side is adjacent to some other region that may or may not be successfully re-labeled previously. A given unlabeled residual region will take the label of the adjacent region that shares the longest common boundary, which is denoted by* $s_{l,max}^{t+\Delta t}$ *. If all regions adjacent to this given residual region are unknown, then this residual region cannot be re-labeled in the current iteration. Iterate this procedure until all unknown residual regions are re-labeled.*

We illustrate the preservation of topological dependence in Fig. 2, in which the nucleus segments are indicated in black and the cell segments in red, blue and green. The dotted line represents the watershed line. Fig. 2(a) shows three cell segments that are topologically dependent with the nucleus segments at time t. Fig. 2(b) shows that when the level set function evolves to time $t + \Delta t$, the connected regions of the zero level set is no longer topologically dependent with the nucleus segments. The gray region that does not contain any nucleus is removed. In Fig. 2(c), the remaining connected regions are separated using the watershed line W^t calculated at the previous time step t. This produces seven connected regions $\beta_1^{t+\Delta t}, \beta_2^{t+\Delta t}, \cdots \beta_7^{t+\Delta t}$. $\beta_1^{t+\Delta t}, \beta_2^{t+\Delta t}$ and $\beta_3^{t+\Delta t}$ contain nucleus segments and are re-labeled according to the corresponding nucleus segments ω_i^n. $\beta_4^{t+\Delta t}, \beta_5^{t+\Delta t}, \beta_6^{t+\Delta t}$ and $\beta_7^{t+\Delta t}$ are re-labeled using the procedure described in **Re-labeling of the residual regions**. Note that $\beta_4^{t+\Delta t}$ is re-labeled with the same integer as $\beta_1^{t+\Delta t}$ because the common boundary $s_1^{t+\Delta t}$ is longer than $s_2^{t+\Delta t}$. After the topological dependence is preserved, the watershed lines are updated according to the new cell segments $\omega_1^{t+\Delta t}, \omega_2^{t+\Delta t}$ and $\omega_3^{t+\Delta t}$ based on Eq. (7).

5 Experimental Results

We applied our segmentation approach to a neural cell study. In this study, we want to automatically and quantitatively measure the length of the neurite. Accurate segmentation of the neural cell is a prerequisite to measure the length of neurites and extract quantitative information on a cell-by-cell basis. As shown in Fig.1, neurites are thin long structures that growth radially outwards from the cells. More than 6000 images are acquired from fixed neural cells with DAPI

stain for nucleus and FITC stain for cell cytoplasm. Zeiss Axiovert 200M wide-field fluorescent microscope of two channels with Motorized XY Stage is applied to capture the cellular images. The original images are captured at 20X magnification with 1366X1020 pixels of 12 bits accuracy. The camera is CoolSnap CCD Camera and the resolution is 0.31 μm/pixel.

It is important to select the proper parameters for cell segmentation, such as Δt in Eq.(3), λ_1 and λ_2 in Eq.(2). We choose a big time step $\Delta t = 10$ to compromise accuracy and computation. To verify that using $\Delta t = 10$ does not introduce significant numerical errors, we performed our segmentations on eight randomly selected images with three different time steps Δt=1, 5 and 10. We use Adjusted Rand Index [24] to compare the segmentations of Δt=1 and Δt=5 with the segmentation of Δt=10. Adjusted Rand Index is 0.9944± 0.0025 for Δt=1 *vs.* Δt=10 and 0.9952±0.0024 for Δt=5 *vs.* Δt=10. Results show that using a big time step does not introduce significant numerical errors. Regarding the regularization parameters, we set $\lambda_1 = 1$ and $\lambda_2 = 50$ for the cell segmentation such that we may preserve the continuity of weakly connected neurites.

We choose the image in Fig. 1(a) and show $\omega_i^{c,t}$ at different time t in Fig. 3. ω_i^n are illustrated by the black regions and their geometrical centers indicated by red dots. Different segments of the cells are shown by random colors. The watershed line is illustrated by black solid lines. The segments of cells $\omega_i^{c,t}$ start from the nucleus segments ω_i^n at $t = 0$ and evolve outwards with a speed related with the variation of image intensity. The watershed lines W^t also evolve with time t dynamically based on the constraint of topological dependence. The final segmentation results of the cellular images in Fig. 1 are shown in Fig. 4. Although the cells are irregular and clumpy, our approach can successfully separate them. 89% of 6000 cellular images can be segmented by our approach within 1 minute on a desktop with 2.0GHz CPU and 1Gb RAM.

In order to testify and validate our approach, we compared our approach with CellProfiler [25] and MetaMorph. CellProfiler is one of the popular cellular image analysis freeware developed by the Broad Institute of Harvard and MIT. MetaMorph is a commercial software specially developed for cellular image analysis by MDS Inc. The parameters for CellProfiler are suggested by the software developers and the parameters for Metamorph are tuned by a service engineer from MDS. 100 images containing a total of 4916 cells were randomly selected from our database. They are segmented by CellProfiler, MetaMorph and our algorithm to generate 300 segmented images. These segmentations were then divided into 15 sets of 20 images each. They were randomly shuffled. Two reviewers grade these segmented images without knowing which algorithm was applied. They marked how many cells are segmented incorrectly. After the blind evaluation, we count the number of incorrectly segmented cells for each approach. The results are shown in Table 1.

Our approach achieved the best performance, which is about 2.5% better than CellProfiler and much higher than MetaMorph. CellProfiler tends to over-segment the cells when the shapes of the nuclei and cells are irregular. MetaMorph seems could not detect fine structures of the neurites.

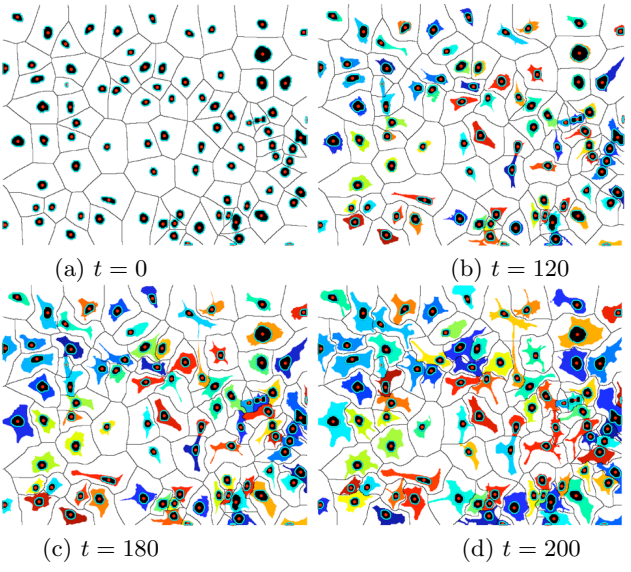

Fig. 3. Dynamical evolution of segments and watershed lines at different time t. Nuclei segments are shown in black and outlined by blue. Their geometric centers are illustrated by red dots. Watershed line are shown by the black line. Different cell segments are indicated by random colors.

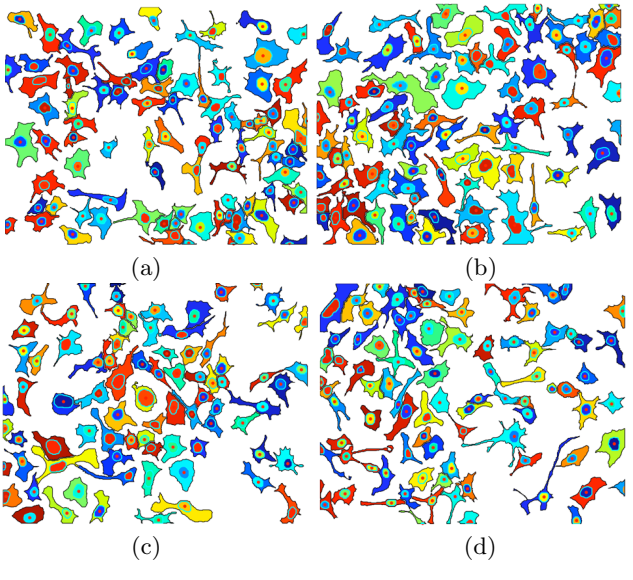

Fig. 4. Segmentation results of our approach. The morphology of the cells in the captured image is complicated. They are clumpy and touched with each other. Our approach can successfully segment them.

Table 1. Comparison of Segmentation Results

Approach	Accuracy
MetaMorph	**74.16%**±1.02%
CellProfiler	**90.85%** ±0.56%
Our Approach	**93.25%** ±0.57%

6 Conclusion

The cell segmentation is non-trivial. It still remains a challenging problem in many bio-imaging informatics applications. Many segmentation algorithms could not properly segment cells that are clumpy and touch each other, especially when the intensity contrast at the boundaries is low and their geometrical shapes are irregular. We proposed a novel segmentation approach for the cellular images captured by two-channel microscope. The proposed approach combines the advantages of level set and watershed method in a novel way based on the concept of topological dependence. Utilization of the dynamics of level set curves in our method is presented for the first time in the literature. Another novelty of our method is that the watershed lines evolve dynamically at each time step t based on the topological dependence, which is essential to prevent merging of cell segments. This constraint also solved the over-segmentation problem of watershed approach. We applied our approach on more 6000 cellular images of neural cells. According to the validation of 100 randomly selected images including 4916 cells, our segmentation method achieved better performance than CellProfiler and MetaMorph. We use only one level set function to segment all the cells in an image, hence our algorithm is more efficient than the work in [18] where each cell is associated with an individual level set function[1].

Segmentation of the cells from the cellular images captured by multi-channel microscope is a common and important problem in many bio-imaging applications. Our approach is developed based on the assumption that the images are captured by two-channel microscope, however, it can be easily generalized and applied to cellular images of multi-channel if the nuclei are captured by one of the channels. Although our approach is not suitable to segment overlapped cells, many biological assays seed and resuspend cells into monolayer such that the cells do not overlap with each other. However, overlapped cells might happen in some other applications and the problem itself is interesting and worth further investigating.

Acknowledgement

The authors would like to appreciate Dr. Anne Carpenter's help to provide the parameters for CellProfiler.

[1] Video demonstrations and Matlab source codes are available at http://web.bii.a-star.edu.sg/∼yuwm/ISVC2008/.

References

1. Choi, W.W.L., Lewis, M.M., Lawson, D., et al.: Angiogenic and lymphangiogenic microvessel density in breast carcinoma: correlation with clinicopathologic parameters and VEGF-family gene expression. Nature, Modern Pathology 18, 143–152 (2005)
2. Bakal, C., Aach, J., Church, C., Perrimon, N.: Quantitative Morphological Signatures Define Local Signaling Networks Regulating Cell Morphology. Science 316, 1753–1756 (2007)
3. Lerner, B., Clocksin, W., Dhanjal, S., Hulten, M., Christopher, M.B.: Automatic signal automatic signal classification in fluorescence in-situ hybridisation images. Bioimaging 43, 87–93 (2001)
4. Lockett, S., Herman, B.: Automatic detection of clustered fluorescence-stained nuclei by digital image-based cytometry. Cytometry Part A 17, 1–12 (1994)
5. Malpica, N., De Solorzano, C.O., Vaquero, J.J., Santos, A., Vallcorba, I., Garcia-Sagredo, J.M., Del Pozo, F.: Applying watershed algorithm to the segmentation of clustered nuclei. Cytometry Part A 28, 289–297 (1997)
6. De Solorzano, C., Malladi, R., Lelievre, S., Lockett, S.: Segmentation of nuclei and cells using membrane related protein markers. Journal of Microscopy 201, 404–415 (2001)
7. Clocksin, W.: Automatic segmentation of overlapping nuclei with high background variaion using robust estimation and flexible contour model. In: Proceedings of 12th International Conference on Image Analysis and Processing, vol. 17-19, pp. 682–687 (2003)
8. De Solorzano, C., Santos, A., Vallcorba, I., Garciasagredo, J., Del Pozo, F.: Automated fish spot counting in interphase nuclei: Statistical validation and data correction. Cytometry Part A 31, 93–99 (1998)
9. Clocksin, W., Lerner, B.: Automatic analysis of fluorescence in-situ hybridisation images. In: Electronic Proceedings of the Eleventh British Machine Vision Conference (2000)
10. Stanley, O., Sethian, J.A.: Fronts propagating with curvature-dependent speed: Algorithim based on hamilton-jacobi formulation. Journal of Computational Physics 79 (1988)
11. Engelking, R.: General topology. Heldermann (1988)
12. Mumford, D., Shah, J.: Optimal approximations by piecewise smooth functions and associated variational problems. Community of Pure Applied Mathematics 42, 577–685 (1989)
13. Chan, T.F., Vese, L.A.: Active contours without edges. IEEE Transactions on Image Processing 10, 266–277 (2001)
14. Tai, X.C., Lie, K.A., Chan, T.F., Stanley, O.: Image Processing Based on Partial Differential Equations. Springer, Heidelberg (2006)
15. Sethian, J.: Level Set Methods and Fast Machining Methods: Evolving Interface in Computational Geometry, Fluid Mechanics, Computer Vision and Material Science. Cambridge University Press, Cambridge (1999)
16. Blum, H.: A transformation for extracting new descriptor of shape. In: Wathen-Dunn, W. (ed.) Models for the Perception of Speech and Visual Form. MIT Press, Cambridge (1967)
17. Tai, X.C., Hodneland, E., Weickert, J., Bukoreshtliev, N.V., Lundervold, A., Ger, H.: Level Set Methods For Watershed Image Segmentation. In: Sgallari, F., Murli, A., Paragios, N. (eds.) SSVM 2007. LNCS, vol. 4485, pp. 178–190. Springer, Heidelberg (2007)

18. Yan, P., Zhou, X., Shah, M., Wang, S.T.C.: Automatic Segmentation Of High-Throughput RNAi Fluorescent Cellular Images. IEEE Transaction on Information Technology in Biomedicine 12(1), 109–117 (2008)
19. Han, X., Xu, C., Prince, J.L.: A Topology Preserving Deformable Model Using Level sets. In: IEEE Computer Society Conference on Computer Vision and Pattern Recognition (CVPR), vol. 2, pp. 765–770 (2001)
20. Zhou, X., Liu, K.Y., Bradblad, P., Perrimon, N., Wang, S.T.C.: Towards Automated Cellular Image Segmentation For RNAi Genome-wide Screening. In: Duncan, J., Gerig, G. (eds.) Proc. Med. Image Comput. Comput.-Assisted Intervention, pp. 885–892. Palm Springs, CA (2005)
21. Whlby, C., Lindblad, J., Vondrus, M., Bengtsson, E., Bjorkesten, L.: Algorithm for Cytoplasm Segmentation Of Fluorescent Labelled Cells. Analytical Cellular Pathology 24(2-3), 101–111 (2002)
22. Xiong, G., Zhou, X., Degterev, A., Ji, L., Wong, S.T.C.: Automated neurite labeling and analysis in fluorescence microscopy images. Cytometry Part A 69A, 495–505 (2006)
23. Bixby, J.L., Pratt, R.S., Lilien, J., Reichardt, L.F.: Neurite outgrowth on muscle cell surfaces involves extracellular matrix receptors as well as ca2+dependent and independent cell adhesion molecules. In: Proceedings of the National Academy of Sciences, vol. 84, pp. 2555–2559 (1987)
24. Hubert, L., Arabie, P.: Comparing Partitions. Journal of the Classification 2, 193–218 (1985)
25. Carpenter, E.A., Jones, R.T., Lamprecht, R.M., Clarke, C., Kang, H.I., Friman, O., et al.: Cellprofiler: image analysis software for identifying and quantifying cell phenotypes. Genome Biology 7 (2006)